View metadata, citation and similar papers at core.ac.uk

brought to you by CORE

provided by IntechOpen

We are IntechOpen, the world's leading publisher of Open Access books Built by scientists, for scientists

4,800
Open access books available

122,000
International authors and editors

135M
Downloads

Our authors are among the

154
Countries delivered to

TOP 1%
most cited scientists

12.2%
Contributors from top 500 universities

CLARIVATE ANALYTICS BOOK CITATION INDEX INDEXED

WEB OF SCIENCE™

Selection of our books indexed in the Book Citation Index in Web of Science™ Core Collection (BKCI)

Interested in publishing with us?
Contact book.department@intechopen.com

Numbers displayed above are based on latest data collected.
For more information visit www.intechopen.com

23

Localized States in Narrow-Gap Ferroelectric-Semiconductor PbSnTe: Injection Currents, IR and THz Photosensitivity, Magnetic Field Effects

Alexander Klimov and Vladimir Shumsky
Rzhanov Institute of Semiconductor Physics, Siberian Branch of RAS
Russia

1. Introduction

For the first time, unusual properties of solid solutions $Pb_{1-x}Sn_xTe$:In with x≈0.24-0.29 (below, PbSnTe:In) were reported in the literature in 1979 (Vul et al., 1979; Akimov et al., 1979). Today, ample experimental data on the properties of PbSnTe:In and theoretical models to explain those properties, and also many reviews of known data for this material (Kaidanov & Ravich, 1985; Volkov et al., 2002), are available. Primary attention was focused on explanation of the following revealed features:

- Fermi-level pinning at the middle of the forbidden band in samples with certain compositions and indium contents, and a low conductivity of the material at temperatures T≤20 K;
- a high photosensitivity of the material: PbSnTe:In readily responds to extremely low radiation fluxes, including those emitted by heated bodies whose temperature only slightly exceeds the sample temperature;
- long-term photosignal decay and residual conduction observed in PbSnTe:In samples after the illumination is switched off.

From the literature (Herrmann & Mollmann, 1983; Vinogradov & Kucherenko, 1991) it was known that in PbSnTe:In samples cooled to temperatures below 20 K spontaneous polarization arises. In the same temperature interval the samples exhibit a pronounced (up to two orders of magnitude) decrease of static dielectric permittivity, whose dependence on temperature yields for the ferroelectric phase transition point a value T_C = 17÷20 K. Like for the well-known isotopic ferroelectric solid solution $(SrTiO_3^{18})_{1-x}(SrTiO_3^{16})_x$ (Mitsuru & Ruiping, 2000), for $Pb_{1-x}Sn_xTe$:In there exists a certain critical value of x such that with less Sn the solid solution behaves as a virtual ferroelectric with a negative temperature T_C while at greater values of x it behaves as an ordinary ferroelectric with temperature T_C dependent on the composition x. Although the occurrence of a "metal–dielectric transition" in PbSnTe:In at temperatures $T \le 20K$ presents a widely recognized fact, manifested as Fermi-level pinning at the middle of the energy gap of PbSnTe:In and resulting in a low (almost intrinsic) concentration of charge carriers in the material, available literature tacitly assumes that in dielectric state no contact injection occurs in PbSnTe samples, and only equilibrium charge carriers define the charge transport in the material. Yet, it was firmly established in

(Akimov et al., 2005) that at helium temperatures in electric fields stronger than about 100 V/cm PbSnTe:In samples become dominated by space-charge-limited injection currents in the presence of electron traps, with the temperature dependence of the current showing a good agreement with calculations performed by the theory of space-charge-limited currents on the assumption of temperature-dependent static dielectric permittivity of the material. It was found that the behavior of static dielectric permittivity as a function of temperature depends on the strength of an electric field superimposed onto the sample, this fact complicating the description of the current versus voltage and temperature (Klimov & Shumsky, 2003). It is clear that with just equilibrium charge carriers taking part in the charge transport the static dielectric permittivity itself and its variation with temperature would not be factors affecting the transport and current-voltage characteristics of the samples.

As stated above, the photoelectric properties of PbSnTe:In at helium temperatures from the very beginning griped fixed attention of researchers; those properties have also triggered many subsequent studies in this field. In steady state, a pronounced sensitivity even to radiation emitted by moderately heated objects with temperatures T = 30÷35 K was observed. In the latter situation, at a working temperature T=4.2 K the photosignal could display decay times ranging from several fractions of millisecond to many hours and even days.

There are several possible explanations to the high photosensitivity and long-term photocurrent relaxation. Until recently, the most frequent explanation rested on an assumption of Yang-Teller (YT) instability that could occur in the crystal surrounding of some point defects in PbSnTe:In; more specifically, it was assumed that an electron capture into some trap could result in lowering of the electronic level of the trap (Volkov & Pankratov, 1980). The electron transition from the conduction band of PbSnTe to the YT center and the reverse transition, electron emission from the center, are thermally activated processes with an activation energy of 0.01 eV, and this leads to a photoconduction decay time increased at T=4 K by a factor of 10^{12} in comparison with the case of no-barrier trapping.

Other alternative explanations were also reported (Vinogradov et al., 1980; Drabkin & Moizhes, 1983) resting on the possibility of emergence, on electron excitation, of a potential barrier that acts to hamper the electron recombination at the level from which the electron was excited by absorbed radiation. The quenching of photoconduction with increasing temperature or following an application of a strong electric-field pulse was normally attributed to increased probability of electron penetration through the potential barrier.

The spectral dependence of photoconduction corresponds to the fundamental absorption band of PbSnTe (band-to-band transitions) (Zasavitskii et al., 1986); nonetheless, photoconduction around wavelengths 115 μm and 220 μm (Romcevic et al, 1991), and also in extended wavelength regions 100 to 200 and around 336 μm, was also reported (Khokhlov et al., 2000; Akimov et al., 2006; Klimov et al., 2007).

In a certain range of applied electric field and illumination intensities, current self-oscillations were observed in PbSnTe (Akimov et al., 1993; Borodin et al., 1997a), which until recently were given no exhaustive explanation.

Recently, the idea about the existence of negative-U centers was revisited by some workers. Possible emergence of the latter situation is described within the frame of two models. In the first, «deformation» model, the energy of a center is defined by the distortion of its nearest crystal surrounding (Volkov & Pankratov, 1980). The second model draws attention to the variable valence of group 3 impurities that may appear in single-charged acceptor state (s^2p^1), in neutral state (s^1p^2), or in single-charged donor state (s^0p^3) (Drabkin & Moizhes,

1981). Those levels are deep; nonetheless, there may also exist shallow levels split from the conduction-band bottom by the Coulomb potential of the center or a system of centers in the state (s^0p^3) (Volkov & Ruchaiski, 1995). As it was noted in (Volkov et al., 2002), both models are capable of providing a reasonable explanation to the effects observed in PbSnTe:In.
Available models, however, disregard the influence the ferroelectric properties of PbSnTe have on the photoelectric phenomena in the material, and the dark conduction and photoconduction in it is not treated in those models with due allowance for the contribution due to contact-injected charge carriers. The change of the slope of the temperature dependence of current at low temperatures was most often attributed to the variation of the energy position of the level due to indium impurities in the band gap without any explanation given to possible reasons for this phenomenon.
The purpose of the present publication is a data analysis and a development of the concept resting on the following basic ideas:

- transport of charge carriers in PbSnTe:In with $x \approx 0.24$-0.29 is defined by contact injection;
- the energy gap of PbSnTe:In contains localized states acting as electron traps;
- the ferroelectric phase transition has a substantial influence on the observed electrical, magnetic, and photoelectric properties of PbSnTe:In and, above all, on the current-voltage characteristics of samples and on the relaxation of conduction-band electrons injected into the material by an electric field or radiation;
- the dielectric state of PbSnTe:In at helium temperatures is related with the compositional disorder of the material as a solid solution.

We believe that the discussion of the listed, still poorly studied points will enable a better understanding of transport phenomena in PbSnTe:In, including the situation in magnetic fields, and will elucidate the role of the ferroelectric phase transition in PbSnTe transport properties.

2. Temperature dependence of conductivity and capacitance, photodielectric effect

2.1 Experimental samples and measurement procedure

We examined PbSnTe:In films MBE-grown on BaF_2 substrates (Klimov & Shumsky, 2001a, 2003). The thickness of the films was about 1 μm, their tin content was $x \approx 0.26$, and the indium content, $\cong$ 3%. For measuring the current-voltage and capacitance-voltage characteristics, special comb structures formed by two metal contacts were prepared. The length of the gap between the contacts was 15 000 μm, and the gap width was 16 to 64 μm. In calculating the capacitance of the structure, the parallel-plate capacitor approximation was used; the applicability of this approximation was justified by the high value of dielectric permittivity, $\varepsilon \geq 400$. For Hall measurements, a standard Hall bar with four potentiometric contacts was employed. The measured sample was contained in a metal chamber that screened it from background radiation.
As the source of radiation, two sources were used. The first source, in what follows to be referred to as the source IR_1, was a small-size incandescent lamp in glass bulb installed directly in the chamber with the sample; this lamp emitted radiation with $\lambda \leq 2$ μm that, following absorption, caused band-to-band transitions in PbSnTe:In. The second source, to be referred to as the source IR_2, was a tungsten incandescent-lamp spiral mounted in an evacuated volume with a polyethylene exit window; behind the window, a combined filter

was installed that allowed only radiation with quantum energies lower than the band-gap energy of PbSnTe:In to come from the volume.

2.2 Experimental data

At low temperatures, T<20 K, at zero voltage in the measurement circuit an electric current was registered; this current could be due to the spontaneous voltage induced in PbSnTe:In by the ferroelectric phase transition (Herrmann & Mollmann, 1983; Nasybbulin et al., 1983; Vinogradov & Kucherenko, 1991; Klimov & Shumsky, 2001b). The strength of the observed current decreased in time below 10^{-14} A, going beyond the measurement accuracy.

At bias voltages below 0.01 V and T=4.2 K without illumination, no direct measurement of sample resistance was possible because the current was too weak (<10^{-14} A). The dark resistance of the sample was therefore evaluated from the proportion between the dark current and the current under illumination, also easily measurable at low voltages, which could be approximated into the interval of low bias voltages. The estimate gave a value greater than 10^{14} Ohm, translating into a specific-resistance value $\rho > 5 \cdot 10^{12}$ Ohm·cm (Klimov & Shumsky, 2001a).

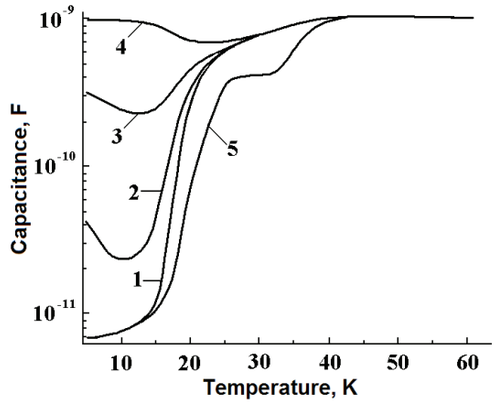

Fig. 1. The curves of sample capacitance versus temperature measured in the dark (1, 5) and under illumination with source IR_1 (2-4). The dc bias voltages are 0 V for curves 1-4 and 1.55 V for curve 5. The voltage supplied to the source, or illumination intensity, increases on going from curve 2 (0.14 V) to curve 4 (1.52 V), the nominal operating voltage of the source being 6 V.

Figure 1 shows the curves of capacitance versus temperature in a sample under zero bias voltage measured in the dark and under illumination, and also a similar curve measured in the dark under dc bias voltage U=1.55 V at frequency f=3.3 kHz (Klimov & Shumsky, 2001a, 2003). A specific feature displayed by the curves is a decrease of capacitance reaching approximately one hundred times on decreasing the temperature from T=25 K to T=15 K without illumination, and also a weak variation of the capacitance in the same temperature interval under illumination. In other words, illumination of the sample at temperatures below 20 - 30 K resulted in increased capacitance of the structure. Another important feature here is the shift towards higher temperatures of the temperature range in which the dark capacitance exhibited strong variations on superimposing a sufficiently strong electric field across the sample. In the latter situation, in the curve of capacitance versus temperature there arises a characteristic shelf in the temperature interval T=25 ÷ 30 K.

In (Vinogradov & Kucherenko, 1991) a similar temperature dependence of capacitance was interpreted as an indication for a ferroelectric phase transition. In our samples, the dependence of inverse dielectric permittivity on temperature has yielded for the Curie point a value T_C=17.5 K under zero bias voltage and a value 19.5 K under bias voltage 1.55 V.
The active and capacitive components of sample conductivity show an increase over the temperature interval from 4.2 to 30 K both during increase of temperature under no-illumination conditions (a) and at fixed temperature during increase of illumination intensity (b). The relation between the concentration of free charge carriers and the sample capacitance in both indicated situations, a and b, for the sources IR_1 and IR_2 proved to be rather intricate.
Figure 2 shows the experimental dependences of the capacitance of structure on its conductance, C=f(σ). It could be expected that, providing that the capacitance variations were defined by the variation of the concentration of free charge carriers in the samples, then, no matter how the latter variation was achieved, the dependence of capacitance versus conductivity would follow one and the same curve in the coordinates σ–C.

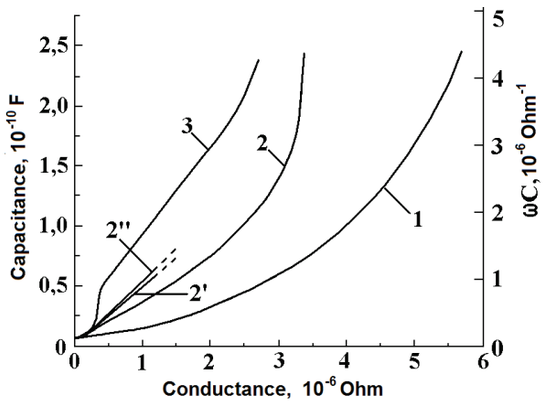

Fig. 2. The proportion between the active conductance of the sample R^{-1} and its capacitance (left axis) or the capacitive conductance (right axis). Frequency f=3.3 kHz. Curve 1 – growth of conductivity and resistance due to increase of temperature from T=4.2 K to approximately T=25 K. Curves 2, 2′, and 2′′ – growth of conductivity under turned-on illumination from source IR_1, 3 – the same with source IR_2. The rise time of conductivity to its maximum value: 2, 3 – 600 s, 2′ – 6 s, 2′′ – 0.4 s. The curve under illumination were measured at T=4.2 K.

However, the relation between the conductivity and capacitance under temperature variations (curve 1) proved to be fundamentally different from that in illuminated sample at liquid-helium temperature (see Figure 2). Moreover, the curve of capacitance versus conductance in the sample illuminated with far-IR source IR_2 (curve 3) was found to show qualitative differences from the curve displayed under illumination with source IR_1 (curves 2, 2′, 2′′). Here, although an increase in illumination intensity from source IR_1 provides for a sharper initial growth of the curve C=f(σ), the slope of this curve tends to saturation, always remaining several times lower than the slope of the similar curve registered with source IR_2.
Measurements of sample capacitance versus the strength of constant electric field superimposed onto sample performed at various temperatures under no-illumination conditions showed that on decreasing the temperature the above dependence became less

pronounced (Klimov & Shumsky, 2001b). Here, in the temperature interval T < 20 K the capacitance behaves non-monotonically as a function of electric-field strength, with an emerging characteristic maximum whose position moves towards higher fields with decreasing temperature.
The shape of the dependences dramatically depends on the rate of change of the electric field (Klimov & Shumsky, 2001b). Under slowly increased field, «quenching of photocapacitance» to the dark level is observed already under electric-field intensities of 400 V/cm. At a rapid sweep of the electric field, the dependences show an intricate behavior with a characteristic peak displayed at E = 400 V/cm. The curves C(V) measured with decreasing electric field differ in shape from the curves registered during an increase of the electric field. Thus, the observed dependences with a capacitance maximum observed at a certain electric-field strength exhibit a non-stationary dynamic pattern.

2.3 Summary

1. The current-voltage characteristics measured under illumination were linear only at low bias voltages (< 0.015 V); the current-voltage curves measured in the dark proved to be linear at even lower voltages.
2. At helium temperatures the films showed a spontaneous voltage typical of ferroelectrics.
3. A photodielectric effect in PbSnTe:In films was observed. This effect consisted in a strong (by two orders of magnitude) increase of low-frequency dielectric permittivity at temperatures below 20 K in samples exposed to electromagnetic radiation. The effect can be attributed to charging processes of impurity centers and to an increase of the effective radii of those centers.
4. A more pronounced increase of capacitance (and dielectric permittivity) was observed in samples exposed to radiation in the fundamental absorption band of PbSnTe:In.
5. The shape of measured curves of capacitance versus field strength was found to be dependent on the rate of change of the field $\partial E/\partial t$.

3. Space-charge-limited currents

3.1 Current-voltage characteristics at T=4.2 K

In «dielectric state», discussed in Introduction, at low concentrations of charge carriers in the allowed bands transport of charge carriers should obey the theory of space-charge-limited currents (Akimov et al., 2005). With traps for charge carriers present in PbSnTe:In, the filling of such traps should have an influence both on the current-voltage characteristics and on the photoconduction relaxation. Experimental structures used for measuring current-voltage characteristics were similar to the structures described in Section 2.1. They were formed by two metal contacts prepared on the surface of PbSnTe:In films. The length of the gap between the contacts was 2 000 to 15 000 μm, and the gap width was 16 to 64 μm. Current-voltage characteristics were measured in the interval of voltages up to 7-8 V using dc sources. In measuring current-voltage characteristics at voltages in excess of 8 V, a generator of rectangular pulses was used to avoid heating of the sample. The pulses followed at time intervals $3 \cdot 10^{-4}$ s, and the width of the pulses was 1, 4, or 8 μs, depending on the voltage range.
Figure 3 shows the current-voltage curve of an PbSnTe:In structure measured at T=4.2 K. In the curve, the following features are distinctly seen: a) a weak growth of the current at a

level of (2-3)·10^{-13} A; b) voltage intervals over which the current shows first a linear and, then, a quadratic growth; c) a transition region; and d) a quadratic dependence of the current on voltage in the range of voltages 20 – 60 V.

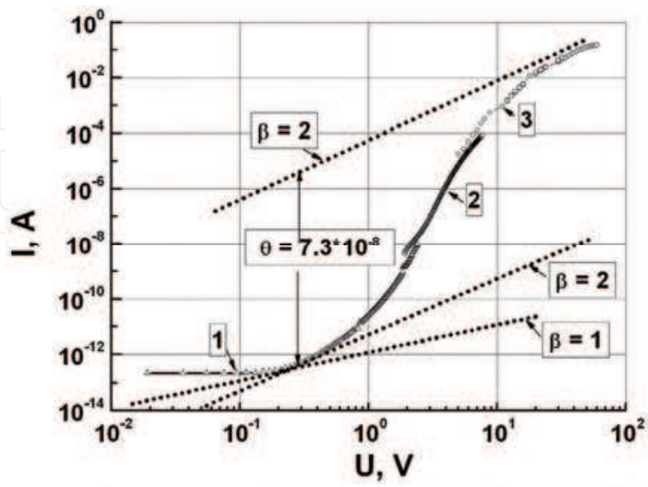

Fig. 3. Current-voltage characteristics of a PbSnTe:In sample at T = 4.2 K. The curves were measured: (1) and (2) - under dc conditions; (3) – in pulsed mode (3).

In the region above U≈0.2 V, the current-voltage characteristics can be understood within the theory of space-charge-limited currents (Lampert & Mark, 1970). The extended transition region with a sharp growth of current over the voltage interval 1 to 10 V points to the presence of various traps in the structure that at U > 20 V become filled with charge carriers. Measurements of current-voltage characteristics at three different widths of the inter-contact gap, 16, 32, and 64 μm, showed that, with decrease of the effective inter-contact separation owing to metal diffusion taken into account, the experimentally measured current values within ±10% obey the proportion $I_1 : I_2 : I_3 = L_1^{-3} : L_2^{-3} : L_3^{-3}$, in line with the theory of space-charge-limited currents.

3.2 Temperature dependence of the current

In the experimental dependences of the current on reciprocal temperature at different voltages (see Figure 4), the following fact is engaging attention: the activation energies ΔE calculated from the relation $i=i_0 exp(-\Delta E/kT)$ at low temperatures have different values at different voltages: the lower the bias voltages, the lower is the activation energy.

Yet, in the temperature region T>20 K the activation energies become roughly identical for all curves. From the standpoint of the theory of space-charge-limited currents, here we have an increase in the concentration of equilibrium electrons, with the ohmic current dominating the conduction. At low temperatures and not too high voltages, when the injection is still weak, deep traps get occupied with electrons, and the activation energy determined from the slope of $i=f(10^3/T)$ gives the trap energy. On increasing the bias voltage in excess of the values at which complete filling of traps occurs ($U > 3 \div 3.5$ V) the electric current becomes weakly dependent on temperature in the temperature region T<10÷20 K. A slight growth of electric current with increasing temperature in this temperature region can be attributed to variation of static dielectric permittivity in the material; this matter will be discussed in

more detail in the next section. Note that, if the dielectric permittivity increases with temperature, at fixed temperature it decreases with increasing the bias voltage. This circumstance affects the observed behavior the electric current shows as a function of temperature at the three bias voltages in Figure 4.

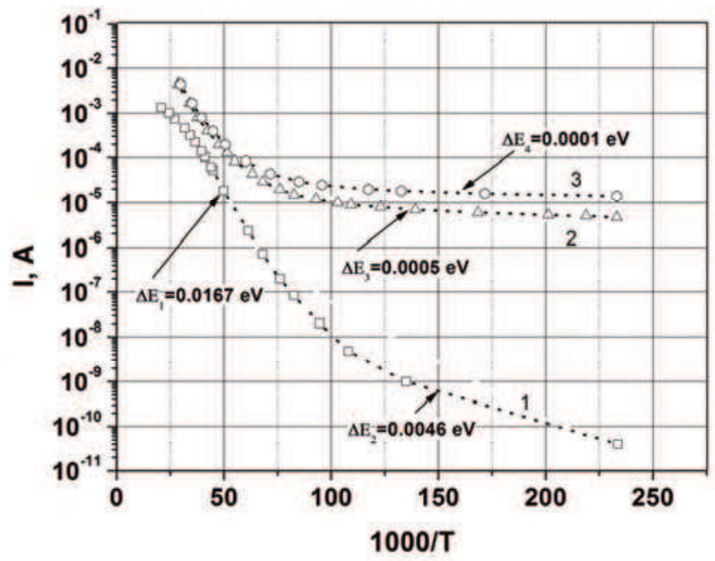

Fig. 4. Temperature dependence of the current through an PbSnTe:In film with x=0.25 under bias voltages 1.55 V (1), 4.65 V (2), and 5.6 V (3). The calculated activation energies are indicated with arrows.

3.3 The energy distribution of traps in the forbidden band of PbSnTe:In

In (Klimov & Shumsky, 2009), current-voltage characteristics were used to extract from them the energy distribution of traps in the forbidden band of PbSnTe:In. The current–voltage characteristics were measured at T = 4.2 K on samples directly immersed into liquid helium and screened from background radiation. A typical characteristic measured on one of the samples is exemplified by Fig. 5.

Following an increase of the bias voltage from 0.7 to 20 V, the electric current increases by more than 13 orders. In a narrow range of bias voltages from 1.82 to 1.92 V the electric current grows in value approximately by four orders. Within the theory of space-charge-limited injection currents, this narrow range of bias voltages can be identified as a range inside which deep traps with a discrete energy level capture electrons to finally become completely filled with them. With further increase of bias voltage, the current grows in value more slowly yet much faster than the quadratic dependence $I \sim U^2$ does. Such a behavior displayed by the current–voltage curves can be attributed to a filling process in which trap levels lying higher in energy than the above-mentioned discrete level become filled with electrons. In the range $U \geq 15$ V, the current tends to follow the dependence $I \sim U^2$, which behavior corresponds to complete filling of all mentioned traps with subsequent limitation of the electric current with the space charge induced in the material by free rather than trapped electrons.

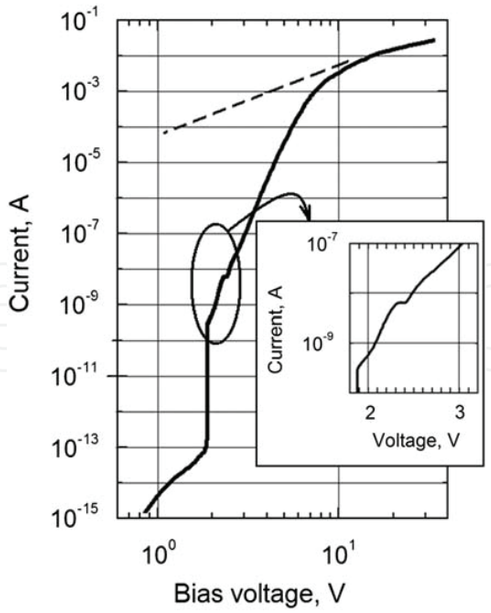

Fig. 5. A current–voltage characteristic measured at T= 4.2 K. Solid line—experiment, dashed line — quadratic dependence for the current.

The energy distribution of electron traps in our samples was calculated under an assumption that the spatial distribution of electrons in between the contacts was uniform, this assumption being a standard one in the theory of space-charge-limited currents. In a biased sample, for the electric current we have:

$$I = q\mu n(U) wd \frac{U}{L}.$$

Here, μ is the electron mobility, and $n(U)$ is the density of free electrons in the material. From here, we readily obtain:

$$n(U) = \frac{IL}{q\mu wdU}.$$

For our sample, the effective density of conduction-band states N_c was calculated as described in (Anderson, 1980); at T = 4.2 K this density was found to equal $N_c \approx 4 \cdot 10^{14}$ cm^{-3}. The calculations showed that in the interval of bias voltages U≤10 V the density of free electrons n(U) was smaller than N_c and, hence, the energy position of the Fermi quasi-level for electrons could be estimated using the simple relation

$$E_{fn} - E_c = kT \ln \frac{n(U)}{N_c}.$$

Under conditions with space-charge-controlled limitation of the electric current, the total charge due to free and trapped electrons is

$$Q = CU = q\left[n(U) + n_t(U)\right] wdL,$$

where C is the experimentally measured capacitance of the structure, and $n_t(U)$ is the density of electrons trapped in the material. Using the values of $n(U)$ and $E_{fn}(U)$, we can determine, from the current–voltage curve, the dependence $n_t = f(E_{fn})$. In an energy interval between E_0 and E, the density of trapped electrons is

$$n_t(E) = \int_{E_0}^{E} g_t(E) f(E) dE,$$

where $g_t(E)$ is the energy distribution of traps in the material, and $f(E)$ is the Fermi–Dirac distribution function. Treating the Fermi–Dirac distribution function as a step function with $f(E) = 0$ at energies $E > E_{fn}$ and $f(E)=1$ at energies $E < E_{fn}$, we can put the upper integration limit equal to E_{fn}. After integration over E_{fn}, we then obtain:

$$g_t(E) = \frac{\partial\left[n_t\left(E_{fn}\right)\right]}{\partial E_{fn}}.$$

The energy distribution of traps calculated by this formula from the experimental current–voltage characteristic is shown in Figure 6. It should be emphasized here that the maxima and minima distinctly observed in the trap spectrum have emerged as a result of an analysis of an accurately measured experimental current–voltage curve. With the adopted algorithm, trap levels below the energy level 0.01 eV from the conduction-band edge could not be reliably identified since this could only be done by accurately measuring the current–voltage curve in the range of currents $I < 10^{-16}$ A.

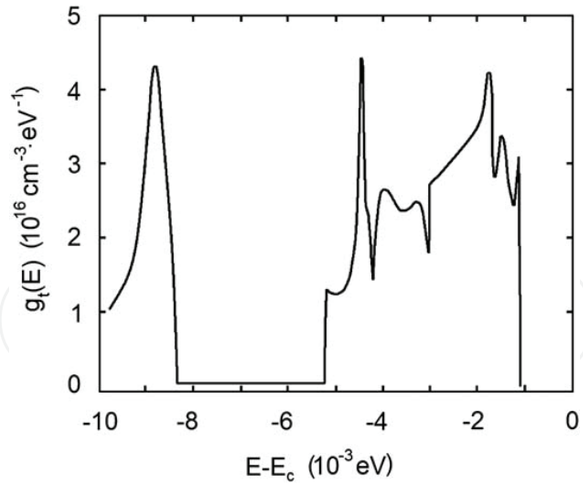

Fig. 6. The energy distribution of traps extracted from measured current–voltage characteristic.

3.4 Summary

The experimental data indicate that in PbSnTe:In samples, in which a «transition to dielectric state» is observed, at helium temperatures the electric current remains ohmic only in weak electric fields. On increasing the field intensity the current becomes limited by the

space charge due to electrons injected from contacts, including trapped electrons. In structures with different separations between the contacts the current varies in inverse proportion to the inter-electrode separation raised to the third power $I \sim L^{-3}$; this finding confirms the applicability of the theory of space-charge-limited currents to PbSnTe:In. An analysis of the temperature dependence of the current at different bias voltages showed that in the coordinates $lgI=f(10^3/T)$ the slope of the curves in the temperature range from 4.2 to 35 K strongly depends on the bias voltage. This observation can be attributed to the fact that, on raising temperature, we have different proportions between the injected and ohmic current. The exact value of this proportion is defined by the behavior of dielectric permittivity as a function of temperature (the dielectric permittivity increases with increasing temperature) and electric-field strength (the permittivity decreases with field intensity). Thus, under conditions with space-charge-controlled limitation of the electric current the slope of the curves $lgI=f(10^3/T)$ depends on the field intensity; this slope can therefore be used for determination of trap activation energies only in weak fields. The aforesaid also applies to interpretation of Hall data.

4. Transport of charge carriers in PbSnTe:In in a magnetic field

4.1 Samples

Experimental type-1 structures (S1) with metal electrodes formed on the surface of PbSnTe:In films of thickness 1 μm were similar to the structures described in Section 2.1; these structures are shown in Figure 7 a. Three orientations of magnetic field with respect to the electric-field direction and the substrate-normal direction were used (Klimov et al., 2009).

The influence of gap orientation in the film plane on the current value was examined on type-2 structures (S2), each structure comprising eighteen 0.2-cm long gaps with 30-μm inter-electrode spacing (see Figure 7 b). In structure S2, each inter-electrode gap was turned through angle 10° in the film plane with respect to the previous gap.

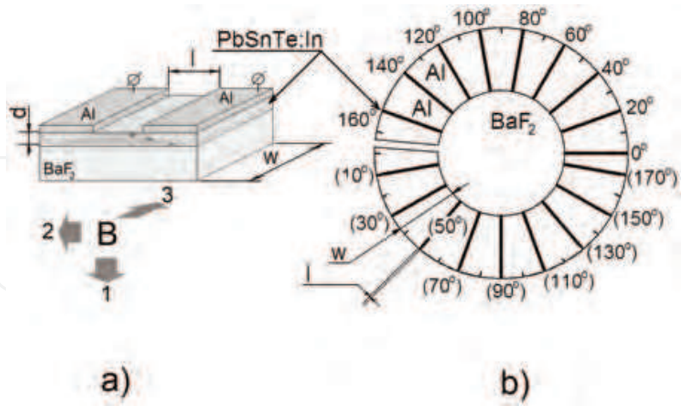

Fig. 7. Experimental structures for examining anisotropic effects in magnetic field. a) inter-electrode gap (d=1 μm, w=0.2 cm, l=30 μm). b) arrangement of eighteen gaps on a single crystal and their angular orientation (the «zero angle» is chosen arbitrarily).

4.2 Current anisotropy in magnetic field

Curves of relative current in magnetic field $I_B/I_{B=0}$ versus bias voltage in an S1 structure are shown in Figure 8 a. The current strength could be increasing or decreasing with bias

voltage depending on mutual orientation of the magnetic and electric fields and the normal to the substrate. Moreover, for orientation 3 the current showed both positive and negative

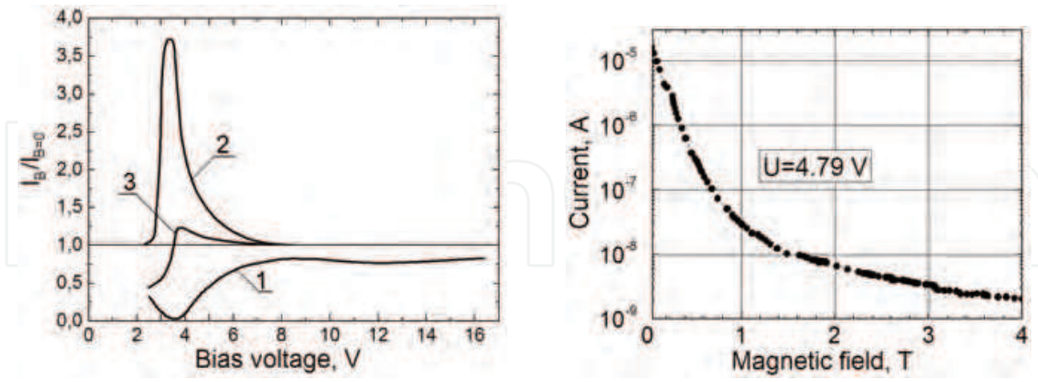

(a) (b)

Fig. 8. a - Curves of relative current versus bias voltage measured at B=0.22 T. Curves 1, 2, and 3 refer to magnetic-field vector orientations indicated in Fig. 4.1 a with the same numerals. b - Curve of electric current versus magnetic-field strength measured at U=4.79 V. Here, the magnetic-field vector was normal to the BaF_2 substrate.

changes with increasing bias voltage. The largest change of current was observed for orientation 1 (Figure 7a). The relative change of current versus magnetic field for this orientation is shown in Figure 8 b. It is seen that at B=4 T the current increases by a factor of 10^4.

Figure 9 shows the angular dependences of the effect at fixed bias-voltage values in magnetic field B=0.22 T at T=4.2 K. On tuning-on and turning-off the field $\overline{B}$, current relaxation over a time 10-30 sec was observed; the relaxation pattern depended on the orientation of the field $\overline{B}$ and on the sample temperature.

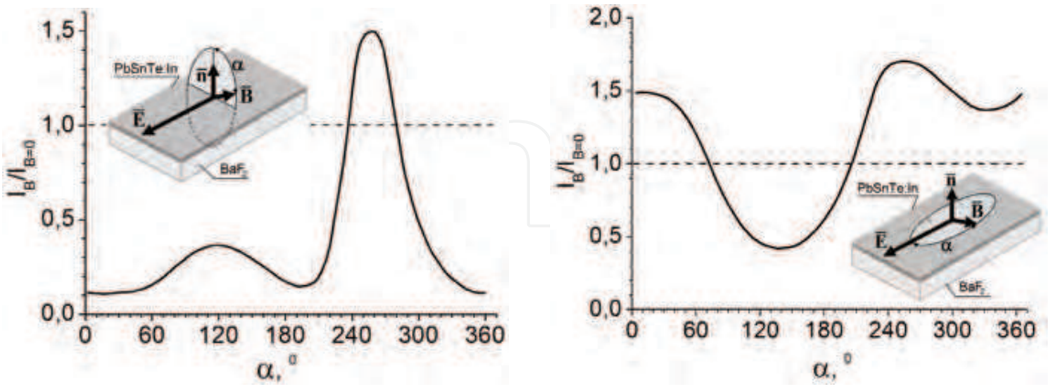

(a) (b)

Fig. 9. a - The electric current versus the angle α between the magnetic-field vector $\overline{B}$ and the normal $\overline{n}$ to the BaF_2 substrate in the plane normal to the electric-field vector $\overline{E}$. b - The electric current versus the angle α between the fields $\overline{B}$ and $\overline{E}$ in the substrate plane. The bias voltages are U=4 V (a) and U=5 V (b).

In the experiment (see Figure 9), the magnetic field was rotated through the angle 360° during 8 minutes so that at each angle a quasi-equilibrium magnitude of the current could establish. Both dependences in Figure 9 show no pronounced angular symmetry. Nonetheless, it is seen from Figure 9 a that two minima of the current lie in the vicinity of the angles 0° and 180°, for which the vector $\overline{B}$ was normal to the substrate. The position of the most pronounced maximum is near the angle 270°, at which the field $\overline{B}$ was normal to the substrate. Yet, the other «local» maximum, located at 120°, is observed rather far from the angle 90°, at which the vector $\overline{B}$ is also parallel to the substrate.
In Figure 9 b the angle between the two maxima is close to 240°, with the «main» minimum being located at the middle point of the maxima with angular spacing of approximately 120° from either maximum. In principle, this position of the three extrema correlates with the orientation of the BaF_2 (111) substrate. Yet, the position of the second «local» minimum shows no such regularity.
The behavior demonstrated by the current in a strong magnetic field also substantially depends on the orientation of this field with respect to the electric-field vector and the normal to the substrate, and it can appear nonmonotonic with variation of $\overline{B}$. Figure 10 shows the curves of relative current for mutual orientation 2 of the two fields (Fig. 7 a) at various bias voltages. The maximum increase in current (over 200 times) was reached approximately at B=1.3 T and at bias-voltage value U≈3 V, i.e. in the vicinity of the voltage at which the effect in weak magnetic fields was also most pronounced (Fig. 8 a)).

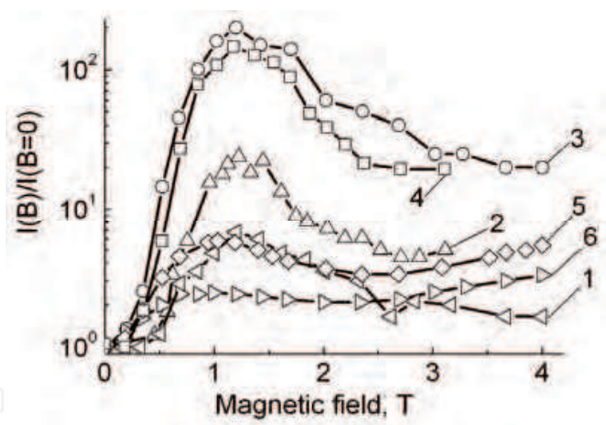

Fig. 10. The ratio I(B)/I(B=0) versus magnetic-field strength. Here, the magnetic field and the electric field are parallel to each other. Bias voltage U, V= 2.66 (1); 2.77 (2); 2.93 (3); 3.1 (4); 4.05 (5); 5.2 (6).

4.3 Discussion

Consider possible factors causing the variation of the electric current under the action of a constant magnetic field. In Section 3 it was shown that at helium temperatures the behavior of current-voltage characteristics of PbSnTe:In films obeys the theory of space-charge-limited current in the presence of electron traps. In the case under discussion, the change of current-voltage characteristics in a magnetic field should be attributed to a change of dielectric permittivity (polarizability) of the medium providing that such a change does take place.

Consider possible change of the effective value of ε as a factor causing variation of the current-voltage curves. Assuming variation of dielectric permittivity by ±30%, we performed numerical calculations of the current-voltage characteristics; the calculated data are shown in Figure 11, curves 1, 2, and 3, together with experimental data. As it is seen from the figure, a good agreement between the calculated and experimental data is observed.

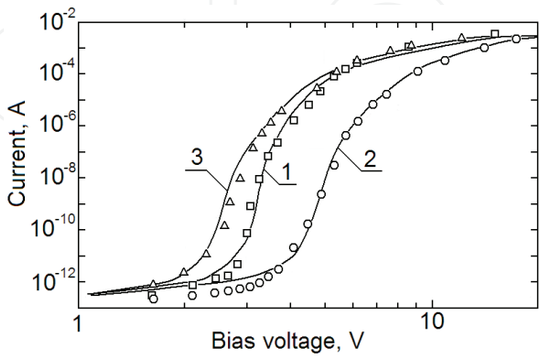

Fig. 11. Current-voltage characteristics of a PbSnTe:In sample at T=4.2 K. Symbols – experimental data; solid lines – calculated data. 1 and squares – B=0, 2 and circles – B = 4 T, orientation 2 in Figure 7 a, 3 and triangles – B = 1.33 T, orientation 2 in Figre 7 a.

Of course, here we do not mean the variation of ε under the action of magnetic field. The magnetic field can alter the current direction by the Hall angle, which in PbSnTe:In can be rather large because of a high value of charge-carrier mobility. In turn, it is the polarizability of the medium in the direction of current that will affect the space-charge magnitude and the current strength, thus making the latter quantities dependent on the direction and strength of magnetic field. If we assume that precisely this factor defines the anisotropic effects in magnetic field, then the dependence of ε on field orientation can also be expected to take place without the magnetic field. To clarify this point, at B=0 we examined the angular dependence of ε and the shape of current-voltage characteristics of structures S2 under conditions with space-charge-controlled limitation of injection current at various orientations of the external electric field.

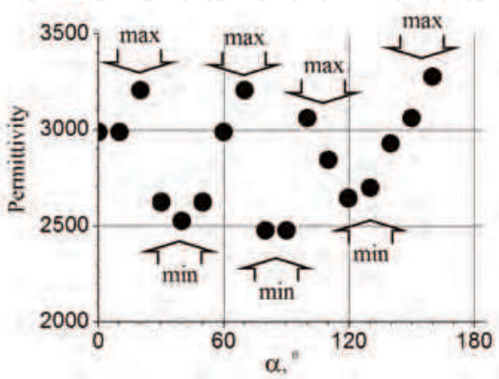

Fig. 12. Dependence of ε on gap orientation in structure S2. The wide arrows indicate the approximate angular position of the maximal and minimal values of ε.

The angular dependence of ε was measured on an experimental structure shown in Figure 7 b. The experimental data measured at frequency f=10^4 Hz are shown in Fig. 12. The dependence shows distinct minima and maxima whose presence in the dependence can be identified by 2 to 4 experimental points within each feature.

The experimentally revealed dependence of ε on electrical-field orientation explains the observed transformation of current-voltage characteristics in a magnetic field. Yet, factors causing the variation of ε need further discussion. At room temperature PbSnTe has a face-centered cubic lattice with the NaCl structure (space group $O_h^5 Fm3m$). As a result of the ferroelectric phase transition, the lattice becomes rhombohedric, involving equivalent [111] spontaneous-polarization axes of «free» crystal. As far as our knowledge goes, so far no data on the dependence of static dielectric permittivity on crystallographic direction in PbSnTe:In have been reported; on the other hand, for thoroughly studied ferroelectrics, such as, for instance, barium titanate, the dielectric-permittivity values measured along directions [010] and [001] form a tensor, whose components in some temperature range can differ by ten to hundred times (Vinogradov & Kucherenko, 1991). The axis along which spontaneous polarization in PbSnTe:In occurs seems to be not parallel to the surface normal, being instead one of the three equivalent type [111] axes directed at an angle to the substrate. The projections of those axes onto the substrate plane are separated with 60° angles. One factor making the indicated three axes nonequivalent on large scale and leading to spontaneous polarization along one of those axes can be some deviation from singularity that inevitably occurs in preparation of BaF_2(111) substrates.

In principle, if spontaneous polarization along one of the three equivalent type-[111] axes does occur, a 60- or 120-deg angular symmetry of the effect in the substrate plane can be expected; such a symmetry is probably manifested in Fig. 9 b. Simultaneously, geometric factors, such as, for instance, a large length of the inter-electrode gap, a small film thickness, and also a multi-domain structure of the film, could also induce distortions into this type of symmetry.

Of course, the model discussed above is a simplified model. In particular, the experimental current-voltage characteristic in substrate-normal magnetic field in Figure 11 and the calculated current-voltage curve can be brought in agreement assuming 30% variation of ε, while measured angular variations of ε are restricted to within 20%. Finally, the model ignores the influence of possible multi-domain structure of PbSnTe:In films on the shape of current-voltage curves, which may appear rather substantial.

4.4 Summary

The giant (up to 10^4) change in the electric current in $Pb_{1-x}Sn_xTe$:In films placed in a magnetic field can be explained within the frame of the following model. The polarizability of PbSnTe:In films in ferroelectric phase at T=4.2 K is anisotropic and, in such films, there exists a preferential direction of spontaneous polarization in which the static dielectric permittivity ε is maximal. The latter assumption is qualitatively corroborated by experimental data on anisotropic properties of the films in zero magnetic field. Since the measured currents are space-charge-limited injection currents, the magnitude of these currents depends on the value of ε in the direction in which the current flows. It can therefore be expected that a magnetic-field-induced change of current direction will alter the magnitude of the current. The observed effect can be explained on the assumption that, on

the change of current direction, the voltage U_t at which the traps in the film become filled with electrons also undergoes a change in the magnetic field, because this voltage is inversely proportional to ε. In a narrow interval of voltages around U_t the electric current increases by several orders. As a result, at a fixed bias voltage even a small change in ε in the above interval will lead to a drastic change of the electric current, this change amounting in the experiments to several orders. Within this model, the complex anisotropy displayed by the effect also receives qualitative explanation. Namely, the magnetic-field-induced increase or decrease of the electric current is defined by the mutual orientation of electric field, magnetic field, spontaneous polarization, and the normal to substrate plane.

5. Photosensitivity of PbSnTe in the fundamental absorption band and in THz spectral region

5.1 Photocurrent in the fundamental absorption band

It is known from literature (Emtage, 1976; Lishka et al., 1984) that the predominant recombination mechanism in undoped PbSnTe samples is Auger recombination. Low concentrations of electrons and holes in PbSnTe:In make the Auger recombination a less probable process. In (Borodin et al., 1997b), it was found that in PbSnTe:In films a satisfactory agreement between experimental and calculated data could be achieved on the assumption that a predominant contribution was due to radiative recombination.

In calculating the photocurrent (Klimov & Shumsky, 2008), it was assumed that the Fermi level under equilibrium conditions lay at the middle of the forbidden band, the concentrations of electrons and holes were negligible, and the concentration of free electrons was defined by the injection current. It was also assumed that there was just one trap level in the material, available in a concentration $5 \cdot 10^{13}$ cm^{-3} and located at energy 0.0065 eV below the conduction-band bottom.

In the dark, in the PbSnTe:In bulk there is an uncompensated negative charge due to electrons, and an injection current flows through the sample. In an illuminated material, optically excited electrons recombine with holes, the role of equilibrium electron concentration here being played by the sum of equilibrium and injected electrons. In performing numerical calculations, the concentration of field-injected electrons in the conduction band and the rate of optical generation of charge carriers were set separately. The total concentration of free electrons defined the energy position of Fermi level and trap occupation values under steady-state conditions. In calculating the Auger lifetime, for the Auger recombination coefficient a value $\eta_n = \eta_p = 5 \cdot 10^{-26}$ $cm^6 \cdot s^{-1}$ was adopted (Emtage, 1976). The radiative lifetime was calculated based on the detailed balance principle (Rooesbroeck & Shockley, 1954).

The temperature dependence of both, Auger and radiative, lifetimes at various contact injection levels is shown in Figure 13 a. At helium temperatures, the chosen minimal total concentration of equilibrium and field-injected electrons refers to the case of almost empty traps, while the maximal total concentration of electrons, to almost completely filled traps (Akimov et al., 2005).

Measurements showed that our PbSnTe:In films were dominated by radiative recombination. Under monopolar electron injection, the hole concentration decreases with increasing injected concentration of free electrons. Illumination produces additional amounts of localized electrons and free holes. Capture of electrons at traps decreases the rate of band-to-band recombination and increases the steady-state hole concentration, thus

increasing the photocurrent value. The calculated electron and hole components of the photocurrent as functions of bias voltage are shown in Fig. 13 b.

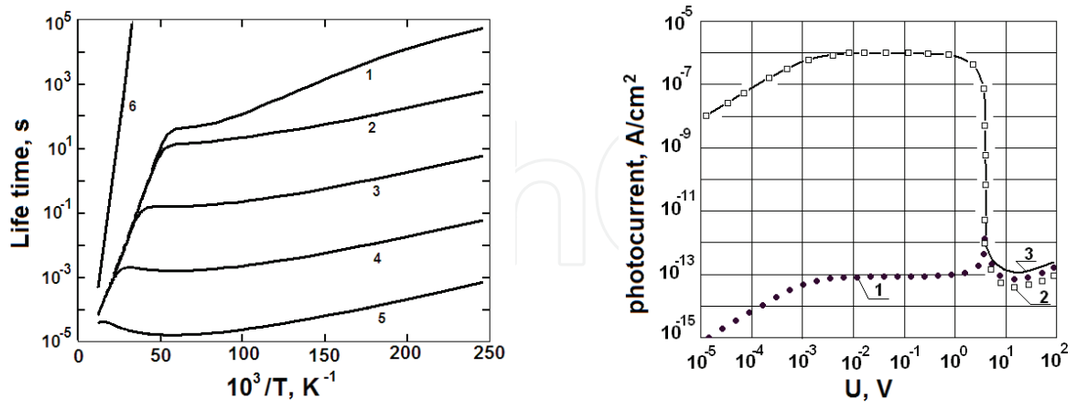

(a) (b)

Fig. 13. Temperature-dependent radiative lifetime (a) and calculated dependences of the photocurrent on bias voltage (b).
a - radiative (1-5) and Auger (6) lifetimes of holes at $\Delta n_{ph}=10^6$ cm^{-3} and $n_0+n_{inj} = 10^6, 10^8, 10^{10}, 10^{12}, 10^{14}$ (curves 1 – 6, respectively).
b - photocurrent component due to electrons (1), due to holes (2) , and the total current (solid line 3) versus bias voltage at $g_0=10$ cm$^{-3}\cdot$s^{-1}.

The prevalence of the hole photocurrent component over an interval of bias voltages up to the voltage at which the traps become filled with electrons is due to the fact that, because of the electron capture at traps, the concentration of free holes here far exceeds the concentration of free electrons. Under such conditions, the hole lifetime is defined by the net concentration of electrons in the conduction band. With further increase of bias voltage, the concentration of conduction-band electrons increases while the lifetime and concentration of optically generated holes start decreasing. In the end, after all traps become filled with electrons, the concentration of excess electrons becomes roughly equal to the concentration of excess holes, and the lifetime of those holes, defined by the concentration of injected electrons. Since the latter concentration is high, the lifetime is short, and the photocurrent is weak.
An important outcome of the calculations is a prediction that until the onset of the regime with completely filled traps the photocurrent should be due to holes.
It was shown experimentally (Klimov & Shumsky, 2008) that in weak fields a hole-type conductivity was observed, with the Hall coefficient being almost independent of bias voltage. In strong fields a current due to electrons is observed, with the Hall effect exhibiting a strong dependence on bias voltage.

5.2 Photocurrent in the THz region

With the previously determined energy distribution of localized centers, the sensitivity of PbSnTn to radiation in submillimeter spectral region due to electron excitation from a center into the conduction band can be calculated (Klimov & Shumsky, 2009). A specific feature of the photocurrent under conditions with space-charge-controlled limitation of current is a strong dependence of photocurrent on the occupation of the local level, this occupation

being in turn dependent on the electron injection level, or bias voltage. This dependence is expected to be manifested most sharply when the trap level lies far from the equilibrium Fermi level. The steady-state concentration of optically generated electrons can be calculated, in principle, similarly to calculations of impurity photoconductivity.

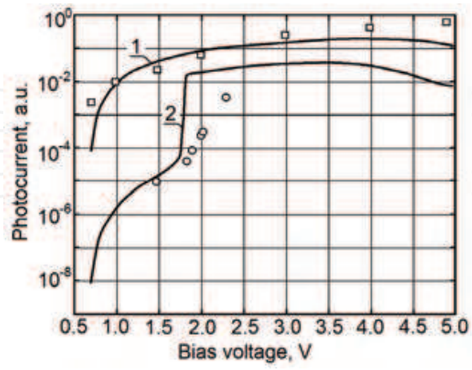

Fig. 14. Current-voltage characteristics of PbSnTe samples illuminated at laser-radiation wavelengths 130 μm (curve 1 – calculated data; squares – experimental data) and 198 μm (curve 2 – calculated data; triangles – experimental data).

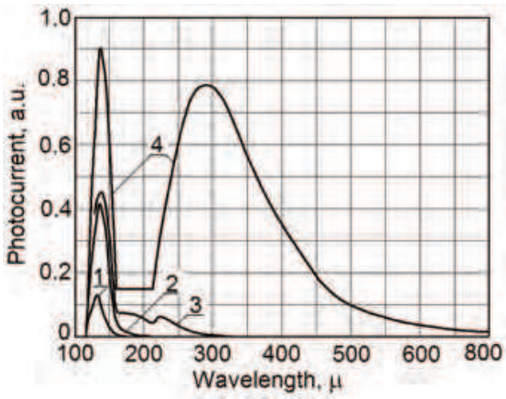

Fig. 15. Spectral dependences of the photocurrent in a structure with an energy distribution of states over the PbSnTe forbidden band shown in Fig. 4, Section 2. U=1.16 (1), 1.79 (2), 1.83 (3), 2.95 V.

The calculated photocurrent values in a sample illuminated with radiation at wavelengths 130 μm (hν=9.54 meV) and 198 μm (hν=6.26 meV) versus bias voltage are shown in Figure 14. The same figure shows the photocurrent values measured in our experiments at the indicated wavelengths.

Figure demonstrates the difference between the curves of photocurrent versus bias voltage for quantum energies hν=9.54 meV and 6.26 meV. In the former case, on increasing the bias voltage from 0.7 V to 5 V the photocurrent varies over an interval of current values slightly in excess of two orders. In the latter case, the photocurrent exhibits variation within the same range of current values on increasing the bias voltage from 1.5 to 2.3 V, the photocurrent growth here being much sharper. Qualitatively, such a behavior complies with the one expected from the energy distribution of states in the forbidden band of PbSnTe.

Calculated values of spectral photosensitivity in a PbSnTe structure under various bias voltages are shown in Fig. 15. It is seen that an increase in the injection level results in a growth of the photocurrent throughout the whole spectral region, this growth being most pronounced at wavelengths λ>200 μm.

5.3 Discussion

The experimental data obtained in our study of photoelectric properties of PbSnTe:In films, and also performed calculations, allow the following conclusions to be drawn:

1. On the passage to «dielectric state», the rate of recombination of optically excited charge carriers becomes predominantly defined by the radiative lifetime, whose magnitude depends on the field-injection level of electrons, on the values of trap parameters, and on the optical injection level.
2. Trapping of optically generated electrons at low field-injection levels leads to prevalence of the photocurrent component due to holes, which on increasing the field-injection level decreases due to recombination of optically excited holes. At high field-injection levels, the photocurrent component due to electrons becomes prevailing. The latter explains the photocurrent quenching by a voltage pulse.
3. The calculated data have found confirmation in measurement of Hall effect in weakly illuminated samples, whose conductivity varies from p-type conductivity at low field-injection levels to n-type conductivity at high field-injection levels.
4. The presence of localized electron traps distributed in energy over the PbSnTe forbidden band may lead to non-exponential photocurrent decay, and also to some other effects such as self-oscillations that were observed, among other things, in Hall effect measurements of weakly illuminated samples.
5. Our calculations of the photocurrent in THz region showed a good agreement with experimental data. Excitation of electrons trapped at energy-distributed localized states in the forbidden band of PbSnTe seems to be capable of providing a reasonable explanation to the high sensitivity of PbSnTe:In films to radiation emitted by weakly heated bodies.
6. Dependence of photosensitivity spectrum in this spectral region on the occupation of traps can be employed in the development of a THz radiation detector controlled by bias voltage applied to the PbSnTe:In structure.

6. Oscillating transient currents in samples screened from background radiation

6.1 Experimental results

Under conditions with screened background radiation at T=4.2 K, we examined the dynamics of injection currents in "dielectric" PbSnTe:In films of thickness 1÷1.5 μm grown by molecular-beam epitaxy on (111) BaF_2 substrates. The specific resistance of the films at T=4.2K was $\rho=10^{10}\div10^{12}$ Ohm·cm. A sample was cooled to T=4.2 K at zero bias voltage, and then a new voltage in the range U=2.5 to 6.0 V was applied to it to register the curve of transient current. At each set value of bias voltage, measurements were repeated thrice. After registration of the first curve (during 40-200 s), the applied voltage was removed from the sample and, after the same time elapsed, the voltage was again applied to the sample to register a second transient-current curve. Then, the sample was "warmed" to a temperature

of 30 K to be again cooled to 4.2 K. Afterwards, the same bias voltage was applied to the sample to register a third transient-current curve.

Figure 16 a, b shows the curves of transient current for bias-voltage values U=2.5 V and U=4.0 V. It is seen that the current in the second measurement was roughly the same as the current at the end of the first measurement; this observation proves that the transition process was over. In the third measurement, the curve of transient current closely followed the curve obtained in the first measurement; the former curve is therefore not shown in the figure. A characteristic feature of the relaxation process was involvement of self-oscillations in the relaxation. The current decay is not monotonic, displaying instead an oscillating behavior. The frequency and amplitude of the oscillations depended on the applied voltage value.

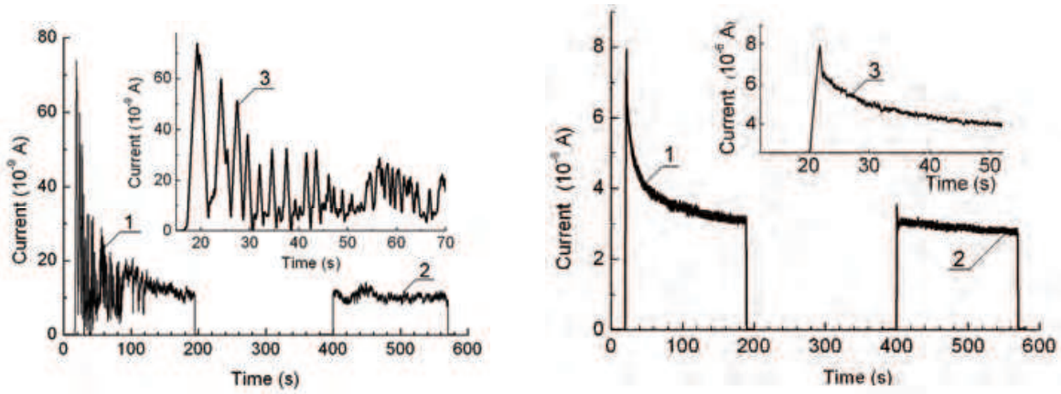

a) b)

Fig. 16. The curves of transient current registered on application of a voltage step to the sample. The bias voltages are U=2.5 V (a) and U=4.0 B (b). The inserts shows the curves of transient current on an enlarged scale.

6.2 Discussion

It is a well-known fact that under certain conditions undamped oscillations can arise in semiconductor structures whose current-voltage characteristics display curve portions with negative differential resistance (NDR). Simultaneously, under certain combinations of external parameters such as temperature, field strength, and illumination intensity, similar self-oscillations were also observed in materials without NDR, for instance, in compensated Si and Ge, and in PbSnTe:In (Akimov et al., 1993).

In applicable theories, the emergence of self-oscillations was related to the occurrence of either trap recharging waves (Suris & Fuks, 1975) or recombination waves in the samples (Bonch-Bruevich & Kalashnikov, 1965); however, in all cases a positive feedback, leading to current growth, was necessary. Such a positive feedback can be ensured by an illumination causing transitions of trapped electrons to the conduction band, collisional ionization of excited electron traps, etc. For instance, according to (Bonch-Bruevich & Kalashnikov, 1965), for emergence of self-oscillations in a unipolar semiconductor the concentration of free charge carriers has to be controlled not only by trapping at one of the centers with a capture cross-section dependent on field intensity, but also by optical generation of free carriers from an impurity level of another type. In our experiments, measurements were carried out

under conditions with background radiation screening, so that the feedback was ensured by some other mechanism.

Previously, we showed (Akimov et al., 2005) that electron transport in semi-insulating PbSnTe:In at helium temperatures cannot be treated without regard for monopolar injection of electrons out of contacts and space-charge-controlled limitation of the current with capture of electrons into localized centers in the forbidden band of PbSnTe. Such an approach has allowed us to explain the shape of current-voltage curves, the high photosensitivity of PbSnTe in the fundamental absorption band, and the emergence of photosignal during excitation of the material in submillimeter band; additionally, an analysis of current-voltage characteristics has allowed us to determine the energy spectrum of localized electron traps (Klimov & Shumsky, 2009). The presence of electron traps and possible recharging of these traps may have an influence on the transition processes. It should be noted that the experimentally observed undamped current oscillations bear no relation to the self-oscillations considered in (Suris & Fuks, 1975; Bonch-Bruevich & Kalashnikov, 1965); the former self-oscillations were observed as an oscillating decay to a steady state after application of a voltage step to the sample. This means that, here, the feedback mechanism, or the mechanism causing an increase of electric current, gradually ceases its operation.

In (Klimov & Shumsky, 2001) we discussed the so-called "photodielectric effect", experimentally observed in PbSnTe:In, that consisted in a considerable (up to two orders) increase of static dielectric permittivity in samples under illumination. This increase can be related to a growth of electronic dielectric susceptibility observed in disordered semiconductors with localization of electrons at discrete levels (Bonch-Bruevich, 1974).

The observed undamped current oscillations can be explained as follows. In the forbidden band of a PbSnTe:In film, there is a quasi-continuous distribution of electron traps; in subsequent discussion, we will treat this distribution by replacing it with a discrete-level set, the levels within the set having different concentrations, energy positions, and electron capture cross-sections. We assume that the steady-state Fermi level is located below the i-th center, and the temperature is sufficiently low for those centers at equilibrium to be empty, for the concentration of conduction-band electrons to be negligible, and for the current through sample to be limited by the space charge and by the trapping of injected electrons at those centers.

On application of a voltage step, injection of an electron concentration $n_{inj}=\varepsilon_0\varepsilon_s U/(qL^2)$ into the sample takes place, where ε_0 is the dielectric constant, ε_s is the static dielectric permittivity of the sample, U is the bias voltage, q is the electron charge, and L is the spacing between the contacts. Consider the variation of the electron concentration in the conduction band and at localized centers starting from a moment $t_0 > \tau_M$, where the latter time is the Maxwell relaxation time. We use an approximation that disregards the diffusion currents and the spatial distribution of electrons over the sample length. Under this assumption, a system of continuity equations with given concentrations and energies of centers can be solved numerically.

Here, a situation may emerge in which a predominant fraction of conduction-band electrons will be first captured by a center with a large capture cross-section, and then the electrons from this center will be emitted into the conduction band to subsequently become trapped at a next center, and so on. Since at an arbitrary time we have $n(t) = n_{inj} - \sum_i m_i(t)$, then the time dependence of the current can be written as

$$j(t) = q\mu n(t)E = \frac{\varepsilon_s \varepsilon_0 \mu U^2}{L^3} - q\mu \frac{U}{L} \sum_i m_i(t) .$$

The above equation shows that the current will decrease in time exhibiting features dependent on the effective time of electron capture into traps up to the establishment of a steady state. Yet, as it follows from (Klimov & Shumsky, 2001), in PbSnTe:In there exist one or several centers which, as they capture electrons, enhance the static dielectric permittivity due to increased electronic dielectric susceptibility. In the latter case, the current is given by

$$j(t) = \frac{\varepsilon_s \varepsilon_0 \mu U^2}{L^3} + q\mu \frac{U}{L} \left[\frac{\varepsilon_0 U}{qL^2} \sum_i \beta_i m_i(t) - \sum_i m_i(t) \right], \quad (1)$$

where β_i is the contribution to polarizability due to one electron captured at the *i*-th center. An analysis of expression (1) shows that at the initial time ($t=t_0$) the current is defined by the first term; at subsequent times, an increase or a decrease of the current is defined by the sign of the bracketed expression. Thus, after application of the voltage step the system can come into a steady state experiencing damped current oscillations. For damped current oscillations to emerge, it is required that the expression in squared brackets would be changing its sign as the centers with a longer time τ_{CM_i} get filled with electrons.

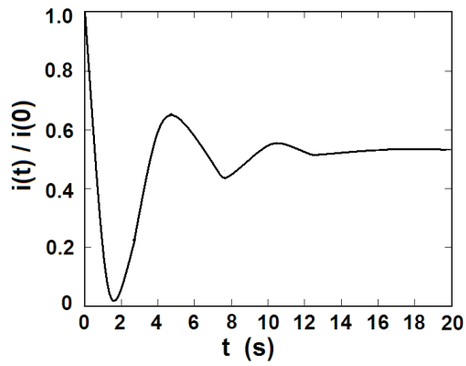

Fig. 17. Calculated current self-oscillations on application of a voltage step U=0.02 V to the sample. The parameter values of the centers are indicated in the text.

The data obtained in numerical calculations of the ratio *j(t)/j(0)* for the model with four discrete levels belonging to centers making different contributions to dielectric susceptibility on electron captures at those levels are shown in Figure 17. The values of trap parameters were chosen rather arbitrarily; they were as follows: $M_1=1.8\cdot10^{12}$ cm^{-3}, $\Delta E_{M1}=4$ meV, $\gamma_1=1.8\cdot10^{-13}$ cm^3/s, $\beta_1=0.5\cdot10^{-9}$; $M_2=1.9\cdot10^{12}$ cm^{-3}, $\Delta E_{M2}=5$ meV, $\gamma_2=6.6\cdot10^{-14}$ cm^3/s, $\beta_2=0.8\cdot10^{-9}$; $M_3=3.0\cdot10^{12}$ cm^{-3}, $\Delta E_{M3}=6$ meV, $\gamma_3=6.3\cdot10^{-15}$ cm^3/s, $\beta_3=1.65\cdot10^{-9}$; $M_4=5.8\cdot10^{12}$ cm^{-3}, $\Delta E_{M4}=8$ meV, $\gamma_4=2.0\cdot10^{-16}$ cm^3/s, and $\beta_4=1.1\cdot10^{-9}$. The numerical values of β_i were chosen such that an increase of current due to increased dielectric permittivity would occur when electrons were getting trapped into the third center in terms of energy.

It is seen from Figure 17 that even involvement of a single such level can lead to damped current oscillations in the trap charging and recharging process. Qualitatively, it is clear that, with the injected electron concentration being much greater than the total concentration of

traps, the charging processes of the various traps will proceed simultaneously without emergence of notable current oscillations. The latter situation refers to the case of high voltages at which a reduction of the current oscillation amplitude and, then, complete vanishing of oscillations were observed in the experiment.
Thus, involvement of the mechanism of current decrease due to trapping-induced reduction of free-electron concentration, on the one hand, and involvement of the mechanism of current increase owing to recharging-induced change of trap polarizability, on the other hand, can result in an oscillating dynamics of the current decay to a steady-state value of the current.

7. Conclusions

The object under study being solid solution Pb-Sn-Te with a substantial (up to a few atomic per cents) In content, this object has to be considered as a disordered system presenting a solid without long-range ordering, with the potential energy of charge carriers no longer being a periodic function of coordinates. The violation of long-range ordering is related to the fact that any chosen site of the metal sublattice may contain, with certain probability, any of the three components. Electronic processes in such systems, namely, in amorphous germanium and silicon, and also in chalcogenide glasses, were considered in (Mott & Davis, 1979). Such properties of PbSnTe:In as the Fermi-level pinning, the absence of an EPR signal, and deviations from linearity in the temperature dependence $\log\sigma = f\left(1/T\right)$ are similar to chalcogenide properties. J. Marshall and A.E. Owen (Marshall & Owen, 1976) considered a state density model assuming that the forbidden band of PbSnTe contains deep donors with energy levels below the acceptor energy (see Figure 18).

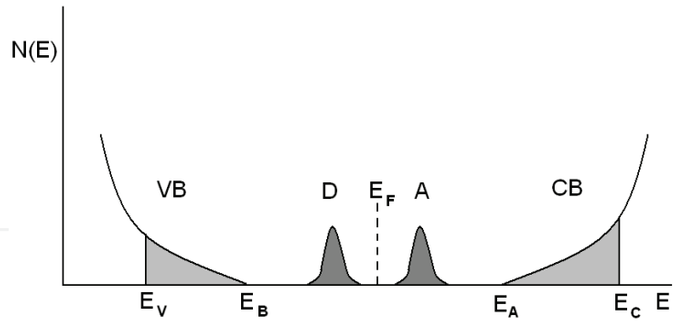

Fig. 18. Density of states in a non-crystalline semiconductor. VB – valence band; CB – conduction band; E_F - Fermi level; D – donors; A – acceptors; E_V, E_C – mobility edges; E_B – valence-band ceiling; E_A – conduction-band bottom. Shaded are localized states.

The states in the forbidden band of PbSnTe pin the Fermi level at the middle of the energy gap, thus leading to decreased conductivity. If the deep acceptor and donor states do not overlap, then unpaired electrons, normally causing an EPR signal, are lacking, except for those due to magnetic impurities. Without going into details, we can state that the model by I.A. Drabkin and B.Ya. Moizhes (Drabkin & Moizhes, 1981) mentioned in Section 1 closely follows the theory by P.W. Anderson (Anderson, 1975).
The unique possibility of creating injecting contacts to PbSnTe:In has allowed researchers to examine charge transport processes related to the recharging phenomena of localized states

in PbSnTe:In both under conditions with screened background radiation and under sample illumination in a broad spectral range, from IR to THz radiation.
The fact that PbSnTe:In is a ferroelectric has widened available possibilities in studying the effect of magnetic field on the charge transport due to electrons.
Of course, the data described in the present publication present no final results; yet, we believe that space-charge-controlled limitation of the electric current, and also capture of electrons into localized traps and their emission from those traps, which affect sample polarizability, are factors that need to be taken into account in developing theoretical models.

8. Acknowledgments

This work was supported by the Programs of Russian Academy of Sciences No. 5.4, 21.20 and, 21.34.

9. References

Akimov A.N., Erkov V.G., Klimov A.E., Molodtsova E.L., Suprun S.P. & Shumsky V.N. (2005). Injection currents in narrow-gap ($Pb_{1-x}Sn_xTe$):In insulators, *Semiconductors,* Vol. 39, No. 5, pp. 533-538, ISSN 1063-7826

Akimov A. N., Erkov V. G., Kubarev V. V., Molodtsova E. L., Klimov A. E. & Shumski V. N. (2006). Photosensitivity of $Pb_{1-x}Sn_xTe$:In films in the terahertz region of the spectrum, *Semiconductors,* Vol. 40, No. 2, pp. 164–168, ISSN 1063-7826

Akimov B.A., Brandt N.B., Bogoslovskii S.A., Riabova L.I. & Choudnev S.M. (1979). Non-equilibrium metal state in $Pb_{1-x}Sn_xTe$(In) alloys. *JETP Letters,* Vol. 29, No. 1, pp. 9-12, ISSN 0021-3640

Akimov B.A., Ryabova L.I., Shumsky V.N. & Petikov N.I. (1993). An operating regime based on switching effect for photodetectors of PbSnTe<In> MBE films, *Infrared Phys.*, Vol. 34, No. 4, pp. 375-378, ISSN 1350-4495

Anderson W. W. (1975). Model for the electronic structure of amorphous semiconductors, *Phys Rev Lett.,* Vol. 34, pp. 953-955, ISSN 0031-9007

Anderson W.W. (1980). Tunnel contribution to $Hg_{1-x}Cd_xTe$ and $Pb_{1-x}Sn_xTe$ p-n junction diode characteristics, *Infrared Phys.*, Vol. 20, pp. 353-361, ISSN 1350-4495

Bonch-Bruevich V.L. (1974). Electronic dielectric susceptibility of a disordered semiconductor, *JETP Letters,* Vol. 19, No. 4, p. 122, ISSN: 0370-274X

Bonch-Bruevich V.L. & Kalashnikov G. *(*1965). On possible recombination instability in semiconductors, *Fizika Tverdogo Tela (in Russian),* Vol. 7, No. 3, pp. 750-758, ISSN 0367-3294

Borodin V.V., Klimov A.E. & Shumsky V.N. (1997). Photocurrent oscillations in PbSnTe<In> films, In: *Narrow Gap Semiconductors,* Shen S.C., Tang D.V., Zheng G.V., Bauer G., pp. 365-368, World Scientific

Borodin V.V., Klimov A.E., Shumsky V.N. (1997). Recombination in PbSnTe <In> at low temperatures, In: *Narrow Gap Semiconductors,* Shen S.C., Tang D.V., Zheng G.V., Bauer G., pp. 361-364, World Scientific

Drabkin I. A. & Moizhes B. Ya. (1981). Spontaneous dissociation of neutral impurity states to positive and negative charge states, *Fizika i Tekhnika Poluprovodnikov (in Russian),* Vol. 15, No. 4, pp. 625-647, ISSN 0015-3222

Drabkin I.A. & Moizhes B.Ya. (1983). On the photoconductivity of $Pb_{1-x}Sn_xTe$ doped with In. *Fizika i Tekhnika Poluprovodnikov (in Russian),* Vol. 17, No. 6, pp. 969-972, ISSN 0015-3222

Emtage P.R. (1976). Auger recombination and junction resistance in lead-tin-telluride, *J. Appl. Phys.,* Vol. 47, No. 6, p. 2565-2576, ISSN 0021-8979

Herrmann K.H. & Mollmann K.-P. (1983). Curie temperature as a critical temperature for dielectric, galvanomagnetic and photoelectrical phenomena in strongly doped $Pb_{1-x}Sn_xTe$. *Phys. Stat. Sol. (a),* Vol. 80, pp. K101-K104, ISSN 0031-8965

Kaidanov V.P. & Ravich Yu.I. (1985). Deep and resonant states in $A^{IV}B^{VI}$-type semiconductors. *Usp. Fiz. Nauk (in Russian),* Vol. 145, No. 1, pp. 51-86, ISSN: 0042-1294

Khokhlov D.R., Ivanchik I. I., Rains S. N., Watson D. M. & Pipher J. L. (2000). Performance and spectral response of $Pb_{1-x}Sn_xTe$(In) far-infrared photodetectors, *Appl. Phys. Lett.,* Vol. 76, pp. 2835-2837, ISSN 0003-6951

Klimov A.E, & Shumsky V.N. (2001). Photodielectric effect in epitaxial Pb1-xSnxTe<In> films produced by molecular beam epitaxy, *Optoelectronics, Insrumentation and Data Processing*, No. 3, pp. 53-62, ISSN 8756-6990

Klimov A.E. & Shumsky V.N. (2001). Giant light-modulated permittivity of $Pb_{0.74}Sn_{0.26}$Te<In> narrow band-gap isolator: new approach to relaxation processes and potential applications, *Proceedings of International Semiconductor Device Research Symposium (ISDRS 2001),* Washington, USA, December 2001

Klimov A. E. & Shumsky V.N. (2003). Photocapacitance effect in narrow band gap PbSnTe<In>, *Proceedings SPIE,* Vol. 5126, pp. 341-346, ISSN 0277-786X

Klimov A., Shumsky V. & Kubarev V. (2007). Terahertz sensitivity of $Pb_{1-x}Sn_xTe$:In, *Ferroelectrics,* Vol. 347, pp. 111-119, ISSN 0015-0193

Klimov A.E. & Shumsky V.N. (2008), Photosensitivity of $Pb_{1-x}Sn_xTe$:In films in the region of intrinsic absorption, *Semiconductors*, Vol. 42, No. 2, pp. 149–15, ISSN 1063-7826

Klimov A., Sherstyakova V. & Shumsky V. (2009). Giant magnetoresistance in narrow-gap ferroelectric-semiconductor PbSnTe:In, *Ferroelectrics*, Vol. 378, pp. 101-110, ISSN 0015-0193

Klimov A.E. & Shumsky V.N. (2009). Shallow traps and the space-charged-induced limitation of the injection current in PbSnTe:In narrow-gap ferroelectric, *Physica B,* Vol. 404, No. 23-24, pp. 5028–5031, ISSN 0921-4526

Lampert M.A. & Mark P. (1970). *Current injection in solids,* Academic Press, N.Y.-London.

Lishka K., Durstberger R., Lindermann G., Staudinger H. (1984). Defect states in $Pb_{1-x}Sn_xTe$, *Phys. Stat. Sol (a).,* Vol. 123, pp. 319–324, ISSN 0031-8965

Marshall J. & Owen A.E., (1976). Field-effect measurements in disordered $As_{30}Te_{48}Si_{12}Ge_{10}$ and As_2Te_3, *Philosophical Magazine,* Vol. 33, p. 457, ISSN 1478-6435

Mitsuru I. & Ruiping W. (2000). Quantum ferroelectricity in $SrTiO_3$ induced by oxygen isotope exchange, *Appl. Phys. Lett.,* Vol. 76, pp. 221–223, ISSN 0003-6951

Mott N.F. & Davis E.A. (1979). *Electron processes in non-crystalline materials,* Clarendon Press. Oxford

Nasybbulin R. A., Girshberg Ya. N., Trunov N. N., Kalimullin R. H., Kukharskii A. A., Kharionovskii Yu. S., Shapkin V. V. & Bursian E. V. (1983). Non-monotone dependence on composition of the ferroelectric phase transition temperature in

$Pb_{1-x}Sn_xTe$, *Fizika Tverdogo Tela (in Russian),* Vol. 25, No. 4, pp. 784–788, ISSN 0367-3294

Romcevic N., Popovic Z.V., Khokhlov D., Nikorich A.V. & Konig W. (1991). Far-infrared study of In doped $Pb_{0,75}Sn_{0,25}Te$ single crystals, *Infrared Phys.,* Vol. 31, No. 3, pp. 225-230, ISSN 1350-4495

Suris R.A. & Fuks B.I. (1975). Sample impedance of compesated material under the conditions of the space-re-charge wave exitation, *Fizika i Tekhnika Poluprovodnikov (in Russian),* Vol. 9, No. 1717-1727, ISSN 0367-3294

Van Rooesbroeck W. & Shockley W. (1954). Photon-radiative recombination of electrons and holes in germanium, *Phys. Rev*., Vol. 94, No. 6, pp. 1558-1560, ISSN 0031-899X

Vinogradov V. S. , Voronova I. D., Kalyuzhnaya G. A. , Ragimova T. Sh. & Shotov A. P. (1980). Hall effect and photoconductivity of $Pb_{1-x}Sn_xTe$ with indium, *JETP Letters,* Vol. 32, No. 1, pp. 20-24, ISSN 0021-3640

Vinogradov V.S. & Kucherenko I.V. (1991). Ferroelectric properties of $Pb_{1-x}Sn_xTe$ (x=0.25) crystals doped with indium. *Fizika Tverdogo Tela (in Russian),* Vol. 33, No. 9, pp. 2572-2578, ISSN 0367-3294

Volkov B. A. & and Pankratov O. A. (1980). Yan-Teller instability of crystal environment of point defects in A^4B^6 semiconductors, *Doklady Akademii Nauk* (in Russian), Vol. 255, No. 1, pp. 93-97, ISSN 0869-5652

Volkov B. A. & Ruchaiski O. M. (1995). Intracenter Coulomb correlations, charge states, and spectrum of group-III impurities in IV-VI narrow-gap semiconductors, *JETP Lett.*, Vol. 62, No. 3, pp. 217-222, ISSN 0021-3640

Volkov B.A., Ryabova L.I. & Khokhlov D.R. (2002). Mixed-valence impurities in lead telluridebased solid solutions. *Physics Uspekhi,* Vol. 45, No. 8, p. 819-846, ISSN 1063-7869

Vul B.M., Voronova I.D., Kaliuzhnaya G.A., Mamedov T.S. & Rakhimova T.Sh. (1979). Peculiarities of transport phenomena in $Pb_{0.78}Sn_{0.22}Te$ with large content of indium. *JETP Letters,* Vol. 29, No. 1, pp. 18-22, ISSN 0021-3640

Zasavitskii I.I., Matvienko A.V., Matsonoshvili B.N. & Trofimov V.T. (1986). Photoconductivity spectrum of $Pb_{1-x}SnxTe$:In epitaxial layers, *Fizika i Tekhnika Poluprovodnikov (in Russian)*, Vol. 20, No. 2, pp. 214-220, ISSN 0015-3222

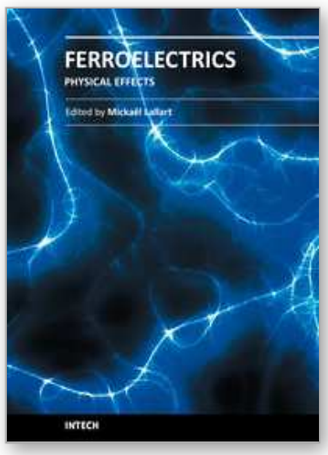

Ferroelectrics - Physical Effects

Edited by Dr. MickaÃ«l Lallart

ISBN 978-953-307-453-5
Hard cover, 654 pages
Publisher InTech
Published online 23, August, 2011
Published in print edition August, 2011

Ferroelectric materials have been and still are widely used in many applications, that have moved from sonar towards breakthrough technologies such as memories or optical devices. This book is a part of a four volume collection (covering material aspects, physical effects, characterization and modeling, and applications) and focuses on the underlying mechanisms of ferroelectric materials, including general ferroelectric effect, piezoelectricity, optical properties, and multiferroic and magnetoelectric devices. The aim of this book is to provide an up-to-date review of recent scientific findings and recent advances in the field of ferroelectric systems, allowing a deep understanding of the physical aspect of ferroelectricity.

How to reference

In order to correctly reference this scholarly work, feel free to copy and paste the following:

Alexander Klimov and Vladimir Shumsky (2011). Localized States in Narrow-Gap Ferroelectric-Semiconductor PbSnTe: Injection Currents, IR and THz Photosensitivity, Magnetic Field Effects, Ferroelectrics - Physical Effects, Dr. MickaÃ«l Lallart (Ed.), ISBN: 978-953-307-453-5, InTech, Available from: http://www.intechopen.com/books/ferroelectrics-physical-effects/localized-states-in-narrow-gap-ferroelectric-semiconductor-pbsnte-injection-currents-ir-and-thz-phot

INTECH
open science | open minds

InTech Europe
University Campus STeP Ri
Slavka Krautzeka 83/A
51000 Rijeka, Croatia
Phone: +385 (51) 770 447
Fax: +385 (51) 686 166
www.intechopen.com

InTech China
Unit 405, Office Block, Hotel Equatorial Shanghai
No.65, Yan An Road (West), Shanghai, 200040, China
中国上海市延安西路65号上海国际贵都大饭店办公楼405单元
Phone: +86-21-62489820
Fax: +86-21-62489821

© 2011 The Author(s). Licensee IntechOpen. This chapter is distributed under the terms of the Creative Commons Attribution-NonCommercial-ShareAlike-3.0 License, which permits use, distribution and reproduction for non-commercial purposes, provided the original is properly cited and derivative works building on this content are distributed under the same license.

IntechOpen

IntechOpen